Synthesis of a new ionic imprinted polymer for the extraction of uranium from seawater

**Hongjuan Zhang · Hele Liang ·
Qingde Chen · Xinghai Shen**

beads [14, 15], silica sol–gel glasses [16], mesoporous IIP material [17] and surface imprinted nanospheres [18, 19]. However, there are only a few studies on the application of IIPs in the recovery of UO_2^{2+} from seawater samples. Singh and Mishra [20] found that the IIP prepared by the ternary complex of UO_2^{2+}- salicylaldoxime-4-vinylpyridine (VP) could quantitatively enrich UO_2^{2+} from dilute aqueous solution at the optimal pH 3.5–6.5. The retention capacity was 0.559 mmol g^{-1}, and the recovery efficiency of uranium(VI) from seawater was 95.9 ± 1.1 %. Shamsipur et al. [21] have prepared a new UO_2^{2+}-IIP coated sorbent, and the recovery of spiked UO_2^{2+} from Caspian Sea water was 103.8 ± 1.8 % at pH 3.0. However, these optimal pHs were not in the pH range of seawater (7.5–8.5).

When the pH of solution is close to that of seawater, the recovery of UO_2^{2+} may be reduced. Metilda et al. [22] found the recoveries of uranium from synthetic seawater (pH = 8.0) using UO_2^{2+}-IIPs prepared with UO_2^{2+}-succinic acid-VP and UO_2^{2+}-5,7-dichloroquinoline-8-ol-VP complexes were 25.0 ± 0.5 and 83.0 ± 0.8 %, respectively. These results seem not so satisfactory resulting from the fact that the uranium is in a strongly complexed form, i.e., uranyl tricarbonate ion $[UO_2(CO_3)_3]^{4-}$, at extreme dilution in the presence of other ions at much higher concentrations, which is the major obstacle to use seawater as an economic source of uranium. To achieve success, the absorbent must work efficiently at the seawater conditions, and must be virtually insoluble [2, 6].

Until now, almost all of the reported IIPs for the pre-concentration and separation of UO_2^{2+} were tested in the $UO_2(NO_3)_2$ solution [20–23]. However, UO_2^{2+} is stable in aqueous solutions in the absence of complexing agents in the pH range from 0 to about 4 [24]. At higher pH value, the UO_2^{2+} may hydrolyze, and generate a series of species such as $UO_2(OH)_2$, $(UO_2)_2(OH)_2^{2+}$ and $(UO_2)_3(OH)^{5+}$ [25], forming colloid or sediment. This may affect the extraction of UO_2^{2+} by IIPs. Hence, it is necessary to study the property of IIP on the extraction of uranium from $[UO_2(CO_3)_3]^{4-}$. However, to the best of our knowledge, there is seldom report so far.

Uranyl ion can be complexed by a variety of ligands at different optimum pH. With respect to β-diketone [26, 27], one kind of wildly used ligands, the optimum pH is close to that of seawater. Hence, an IIP for the selective removal of UO_2^{2+} from $(NH_4)_4[UO_2(CO_3)_3]$ solution was designed using the synthesized ligand 2,4-dioxopentan-3-yl methacrylate with both a β-diketone structure and a methacryloyl group. The methacryloyl group can crosslink the monomer into the polymer matrix, improving the reusability of IIP. The objective of this study is to investigate the influence of the carbonate ions (CO_3^{2-}) on the sorption process and the possible application of this IIP for the recovery of uranium from seawater.

Ex erimental

Reagents and materials

$UO_2(NO_3)_2 \cdot 6H_2O$ (G.R., Chemapol, Prague Czechoslovakia), 3-chloro-2,4-pentanedione (98 %, Acros) and ammonium carbonate (($NH_4)_2CO_3$, A.R., Beijing Yili Fine Chemical Products Inc., China) were used as received. Methacrylic acid (A.R., Beijing Yili Fine Chemical Products Inc., China) and ethylene glycol dimethacrylate (EGDMA, 98 %, Acros) was purified by vacuum distillation before use. Seawater sample was collected from Qingdao coast of China by ud20001((A.R.,)(rece)13(was)001(th-534

4-pentanedione (1 mmol) was added and the mixture was stirred for 4 h at room temperature. After removing the generated inorganic salts by suction filtration, the excess acetone was evaporated by vacuum rotary evaporation, then the residue was washed by diethyl ether and petroleum ether. Finally, it was purified by passing through a column of silica gel and eluted with the eluent of ethyl acetate and petroleum ether (1:12), and a red oil was obtained. ^{1}H NMR, elemental analysis and mass spectra revealed that the oil was the target product, i.e., 2,4-dioxopentan-3-yl methacrylate. ^{1}H NMR (300 MHZ, CDCl$_3$, Me$_4$Si): δ_H 2.02 (s, 3H, CH$_3$), 2.34 (s, 6H, CH$_3$), 5.76 (s, 1H, C=CH), 6.32 (s, 1H, C=CH), 5.55 (s, 1H, CHO). Elemental analysis: calcd (%) for C$_9$H$_{12}$O$_4$ (184.19): C 58.69, H 6.57; found: C 57.90, H 6.54. HRMS: m/z (%): calcd for M+H$^+$: 185.08084, M+Na$^+$: 207.06278; found: M+H$^+$: 185.08077, M+Na$^+$: 207.06249.

Synthesis of ionic imprinted polymer

In 10 mL 1,4-dioxane, 0.50 g (1 mmol) UO$_2$(NO$_3$)$_2$·6H$_2$O was complexed by 3 mmol (0.55 g) 2,4-dioxopentan-3-yl methacrylate. Then, 16 mmol (3.17 g) EGDMA and 20 mg 2,2′-azobisisobutyronitrile were added. The above solution was purged with high-purity N$_2$ for 30 min, then sealed and polymerized in an water bath at 70 °C for 24 h. After being dried at 70 °C to remove the solvent (porogen), the bulk polymers were ground and sieved to get the particles between 80 and 200 mesh. Unreacted monomers were removed by washing with acetone, the mixture of acetone and water, and water in sequence. UO$_2^{2+}$ was leached using successive stirring of particles in 50 mmol L^{-1} HCl solution until the uranium in the leaching solution was hardly detected by ICP-AES. The obtained polymer particles were washed thoroughly by water until the eluent was neutral, and was dried in an oven at 70 °C. The synthesis of UO$_2^{2+}$-IIP is schematically represented in Fig. 1. Control polymer (CP) particles were prepared under similar conditions except the absence of UO$_2^{2+}$.

Retention capacity studies

The maximum amount of preconcentrated UO$_2^{2+}$ of the material (retention/binding capacity of IIP or CP) was determined by saturating 10 mg polymer particles with 10 mL uranium(VI) solution (the initial uranium concentrations of (NH$_4$)$_4$[UO$_2$(CO$_3$)$_3$] and UO$_2$(NO$_3$)$_2$ solutions are 2–20 and 4–40 mg L^{-1}, respectively) under the preset conditions. After adsorption, the concentration of UO$_2^{2+}$ in the mother solution was measured by ICP-AES.

The equilibrium adsorption capacity (Q_e, mg g^{-1}) was calculated by Eq. 1.

$$Q_e = (C_0 - C_e)V/W \tag{1}$$

where C_0 and C_e (mg L^{-1}) are the initial and equilibrium concentrations of adsorbate, respectively. V (mL) is the volume of the testing solution and W (g) is the weight of sorbent. Then, the corresponding adsorption isotherms were obtained.

Selectivity studies

The inorganic ions for selectivity studies were Li$^+$, Na$^+$, K$^+$ and Rb$^+$. The selectivity experiment of UO$_2^{2+}$-IIP and CP for uranium(VI) over other inorganic ions was carried out by stirring 10 mL aqueous solution containing 10 mg polymers and 100 μg each individual inorganic ion under identical conditions. The concentrations of these ions in mother solution were measured by ICP-AES after adsorption.

The relative selectivity coefficient k' was calculated according to Eq. 2.

$$k' = S(\text{IIP})/S(\text{CP}) \tag{2}$$

where $S(\text{IIP})$ and $S(\text{CP})$ represent the selectivity coefficient of UO$_2^{2+}$-IIP and CP, respectively. The selectivity coefficient S is defined by Eq. 3.

$$S_{U/M} = D_U/D_M \tag{3}$$

where D_U and D_M are the distribution ratios of the UO$_2^{2+}$ and other inorganic ions, i.e., Li$^+$, Na$^+$, K$^+$ and Rb$^+$, with polymers (IIP/CP), respectively. These distribution ratios were calculated using Eq. 4.

$$D = (C_0 - C_e)V/C_eW \tag{4}$$

where C_0 and C_e (mg L^{-1}) represent the initial and equilibrium concentrations of the given metal ions in solution, respectively.

Results and discussion

Characterization of IIP and CP

FT-IR spectra

The FT-IR spectra of the CP, IIP and unleached IIP show a similar backbone beacacuse of a high level of EGDMA, the cross linking reagent were used (Fig. 2). All three spectra show a strong absorption peak at 1,728 cm^{-1} attributed to the stretching vibration of C=O group and the other distinctive peak at 1,153 cm^{-1} assigned to the stretching vibration of C–O group [29]. The absorption at 1,637 cm^{-1} attributed to the stretching vibration of C=C group is almost diminished in all polymers, indicating that almost

Fig. 1 Scheme for the preparation of UO_2^{2+}-IIP
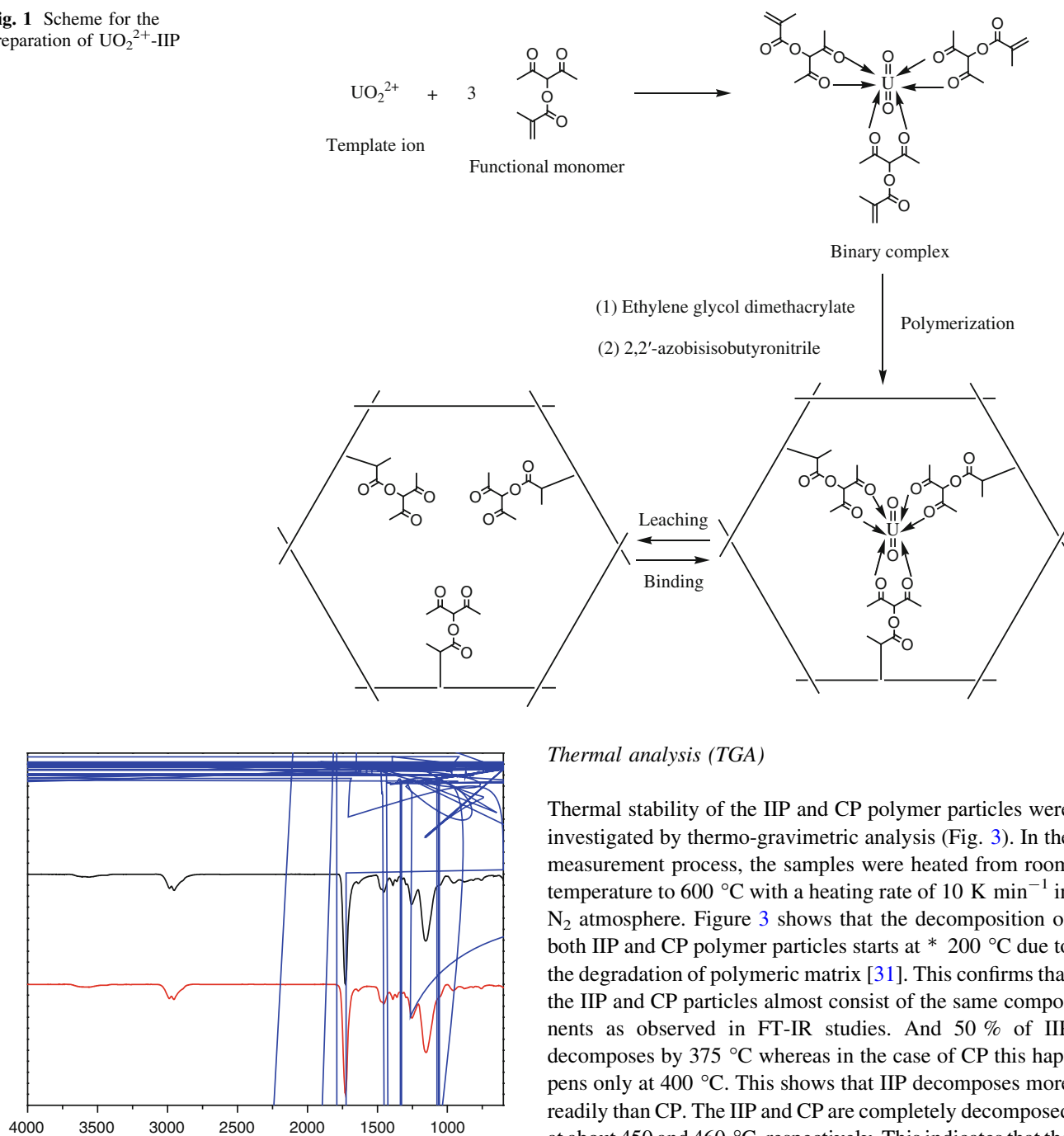
Thermal analysis (TGA)

Thermal stability of the IIP and CP polymer particles were investigated by thermo-gravimetric analysis (Fig. 3). In the measurement process, the samples were heated from room temperature to 600 °C with a heating rate of 10 K min^{-1} in N$_2$ atmosphere. Figure 3 shows that the decomposition of both IIP and CP polymer particles starts at * 200 °C due to the degradation of polymeric matrix [31]. This confirms that the IIP and CP particles almost consist of the same components as observed in FT-IR studies. And 50 % of IIP decomposes by 375 °C whereas in the case of CP this happens only at 400 °C. This shows that IIP decomposes more readily than CP. The IIP and CP are completely decomposed at about 450 and 460 °C, respectively. This indicates that the CP particles are more rigid than the IIP particles due to a lot of hollow sites existing in the latter after leaching out UO_2^{2+}.

Surface area analysis

With respect to adsorption materials, the surface area is an important parameter. Generally, it is believed that materials with larger surface area have higher adsorption capacity [17, 32, 33]. Herein, the BET surface areas of UO_2^{2+}-IIP

all the monomers were polymerized [30]. The absorption peak at 920 cm^{-1} corresponding to the asymmetric stretching vibration of U=O group in UO_2^{2+} is only observed in the unleached IIP (curve a, Fig. 2) and disappeared in IIP (curve b, Fig. 2).
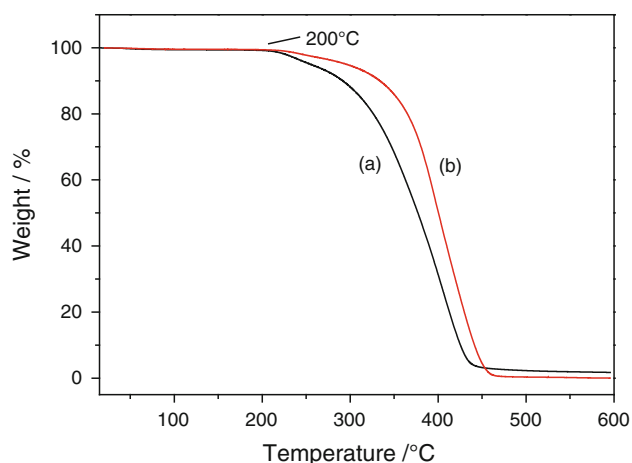
Fig. 3 TGA plots of IIP (a) and CP (b) particles

and CP are measured to be 97.37 and 143.18 m^2 g^{-1}, respectively.

Kinetics of uranyl ions adsorption

The equilibrium time of adsorption of UO$_2$$^{2+}$ from aqueous solutions was determined (Fig. 4a). As seen, the initial adsorption of UO$_2$$^{2+}$ by the polymer particles is fast, then it gradually reaches a plateau.

To evaluate the adsorption kinetics of UO$_2$$^{2+}$, two different kinetic models were applied to fit the experimental data: (1) the pseudo-first-order kinetic model; (2) the pseudo-second-order kinetic model, which can be expressed as linear forms by Eqs. 5 and 6, respectively [34].

$$\ln(Q_e - Q_t) = \ln Q_e - k_1 t \tag{5}$$

$$t/Q_t = 1/(k_2 \cdot Q_e^2) + t/Q_e \tag{6}$$

where Q_e (mg g^{-1}) is the adsorption capacity at equilibrium, Q_t (mg g^{-1}) is the adsorption amount at time t (h), k_1 (h^{-1}) and k_2 (mg g^{-1} h^{-1}) are the adsorption rate constants related to pseudo-first-order and pseudo-second-order kinetic models, respectively.

To compare the validity of each model, a normalized standard deviation ΔQ_e (%) was calculated using Eq. 7 [35].

$$\Delta Q_e = \sqrt{\frac{\Sigma |(Q_{exp} - Q_{cal})/Q_{exp}|^2}{N - 1}} \times 100\% \tag{7}$$

where Q_{exp} and Q_{cal} (mg g^{-1}) are the experimental and calculated amount of UO$_2$$^{2+}$ adsorbed on IIP or CP, respectively, and N is the total number of measurements. If the calculated data in a model are close to the experimental data, the value of ΔQ_e (%) will be lower. Otherwise, the value of ΔQ_e will be higher. All kinetic parameters, correlation coefficient (R^2), and ΔQ_e are listed in Table 1. It
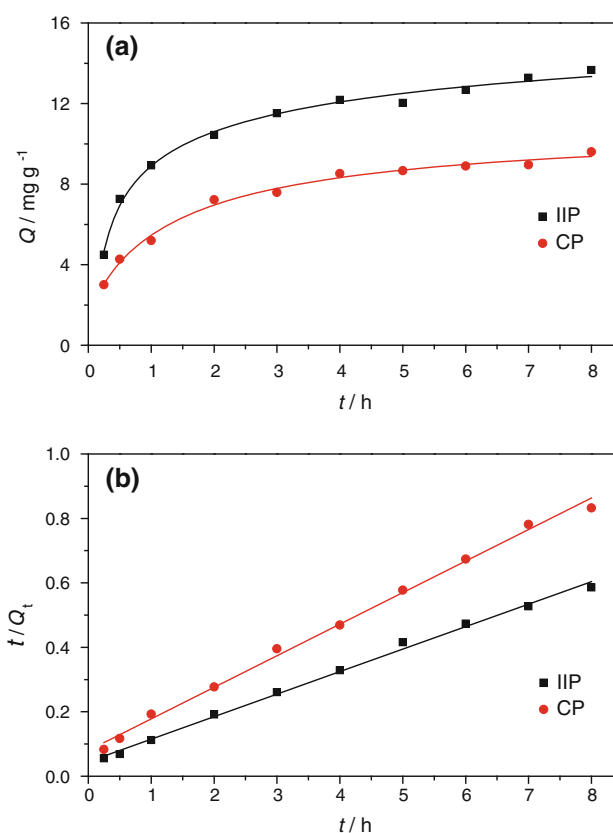

Fig. 4 Effect of time on the adsorption of UO$_2$$^{2+}$ (**a**) and plots for pseudo-second order kinetic modeling (**b**). (Adsorbent: 10 mg, uranium concentration: 20 mg L^{-1}, uranium solution: 10 mL, temperature: 25 °C)

can be seen that the adsorption of UO$_2$$^{2+}$ onto IIP and CP does not follow the pseudo-first-order kinetic model with lower R^2 and higher ΔQ_e. On the contrary, the results present an ideal fit to the pseudo-second-order kinetic model (Fig. 4b) with high R^2 and low values of ΔQ_e. Furthermore, the values of Q_{exp} access those of Q_{cal}, inferring that the adsorption equilibrium was almost achieved within 8 h. In order to ensure the arrival of adsorption equilibrium, the adsorption time was chosen to be 9 h in the further studies.

Retention capacity studies

In the studied concentrations, the adsorption capacity of the polymer particles rises with the increase of uranium concentration until it reaches saturation. The maximum retention capacities of IIP and CP polymer particles are 15.3 and 11.2 mg g^{-1} in (NH$_4$)$_4$[UO$_2$(CO$_3$)$_3$] solution (Fig. 5a), respectively. The retention capacities of IIP are higher than that of CP at all initial concentrations of uranium(VI). This observation demonstrates that specific binding sites are created within the polymeric matrix that increases the affinity of the IIP toward UO$_2$$^{2+}$. It is the

Table 1 Comparison of the fitting results of the pseudo-first-order and pseudo-second-order kinetic models

	Q_e(exp) (mg g^{-1})	Pseudo-first-order kinetic model				Pseudo-second-order kinetic model			
		k_1 (h^{-1})	R^2	Q_e(cal) (mg g^{-1})	ΔQ_e (%)	k_2 (mg g^{-1} h^{-1})	R^2	Q_e(cal) (mg g^{-1})	ΔQ_e (%)
IIP	13.7	0.390	0.9406	7.99	41.7	0.108	0.9961	14.3	4.38
CP	9.61	0.354	0.9549	5.94	38.2	0.120	0.9957	10.2	6.14

existence of imprinted sites with a large amount that leads to the selective adsorption of UO_2^{2+} and the improvement of the adsorption capacity. However, the sites in CP do not match UO_2^{2+}, reducing its retention capacity. Therefore, although the surface area of IIP is lower, its adsorption capacity for UO_2^{2+} is higher. It can be concluded that the binding ability and selectivity of imprinted polymers are independent on their surface area [18, 36].

The maximum retention capacities of IIP and CP in $UO_2(NO_3)_2$ solution are 23.9 and 23.3 mg g^{-1} (Fig. 5b), respectively. The capacity of IIP in $(NH_4)_4[UO_2(CO_3)_3]$ solutions is lower than that in $UO_2(NO_3)_2$ solutions at the higher initial uranium concentrations, which is opposite in the case of lower initial uranium concentrations. However,

the capacity of CP in $(NH_4)_4[UO_2(CO_3)_3]$ solutions is lower than that in $UO_2(NO_3)_2$ solutions at all initial uranium concentrations. In the prepared $(NH_4)_4[UO_2(CO_3)_3]$ solution, there is a large amount of free CO_3^{2-} ions, making the solution stable. However, just these CO_3^{2-} ions increase the pH value of the solution, and compete with β-diketone groups to combine with UO_2^{2+} ions, leading to the reduction of the retention capacity for UO_2^{2+}. With respect to CP, this effect is larger than that for IIP. Furthermore, the effect of CO_3^{2-} concentration on the adsorption of UO_2^{2+} in $(NH_4)_4[UO_2(CO_3)_3]$ solution was studied (Fig. 6). It can be seen that the adsorption capacity of the polymer particles decreases with the increase of CO_3^{2-} concentration. When the CO_3^{2-} concentration reaches 8 mmol L^{-1}, the IIP cannot adsorb UO_2^{2+} any more. In the literature, the concentration of CO_3^{2-} in the seawater is estimated to be 2 mmol L^{-1} [37]. Herein, the prepared IIP still kept a good adsorption capacity for UO_2^{2+} at this CO_3^{2-} concentration. This suggested that the IIP has the ability to extract UO_2^{2+} from seawater.

The adsorption of UO_2^{2+} from $(NH_4)_4[UO_2(CO_3)_3]$ aqueous solution onto IIP at various temperatures is shown in Fig. 5a. With the increase of temperature from 288 to 298 K and to 308 K, the Q_e values of IIP are elevated
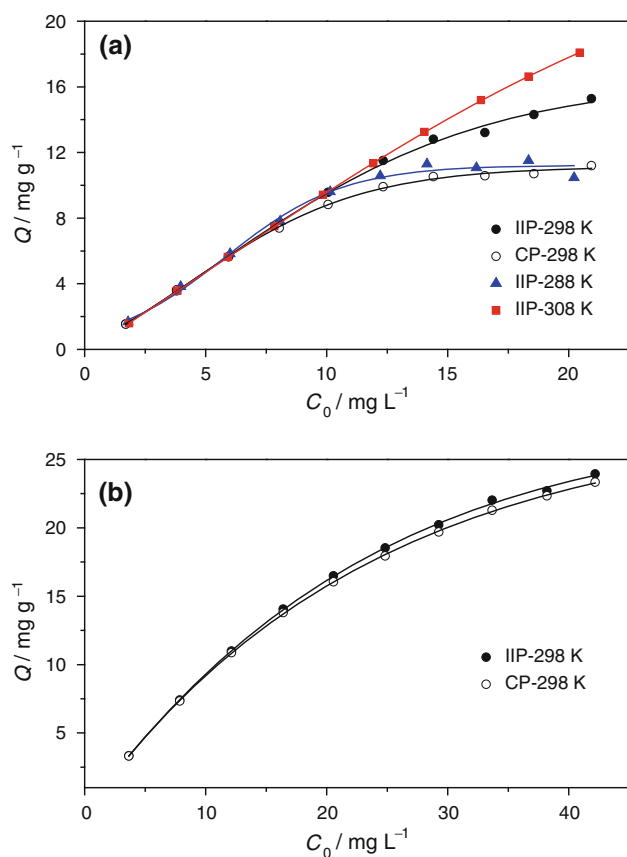
Fig. 5 Effect of UO_2^{2+} concentration on the adsorption of UO_2^{2+} in $(NH_4)_4[UO_2(CO_3)_3]$ (a) and $UO_2(NO_3)_2$ (b) solutions. (Adsorbent: 10 mg, adsorption time: 9 h, uranium solution: 10 mL)
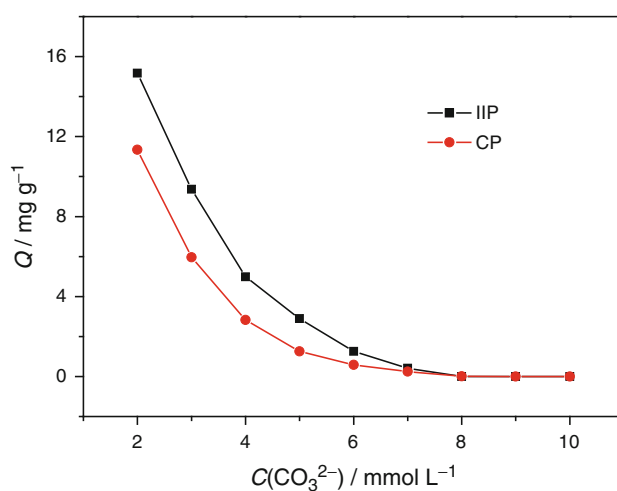
Fig. 6 Effcet of CO_3^{2-} concentration on the adsorption of UO_2^{2+} in $(NH_4)_4[UO_2(CO_3)_3]$ solution. (Adsorbent: 10 mg, adsorption time: 9 h, uranium concentration: 20 mg L^{-1}, uranium solution: 10 mL, temperature: 25 °C)

Table 2 Selective adsorption properties of the IIP and CP

Ion	D_U		D_M		$S_{U/M}$		k'
	CP	IIP	CP	IIP	CP	IIP	
Li^+	7.5	25	0.20	0.18	38	140	3.7
Na^+	5.6	18	0.25	0.20	22	90	4.1
K^+	6.1	20	0.27	0.26	23	77	3.3
Rb^+	7.1	26	0.37	0.30	19	87	4.6

obviously. The possible reason is that the high temperature promotes UO_2^{2+} to pass the external boundary layer, and produce the enlargement of pore volume and surface area, making UO_2^{2+} penetrate the inner of IIP more easily [38].

Selectivity studies

The distribution ratio and selectivity coefficients of IIP and CP for UO_2^{2+} over other inorganic ions are shown in Table 2. The selectivity coefficients of IIP are greater than that of CP owing to the size and shape specific cavities created in IIP, i.e., imprinting effect. Based on the results shown in Table 2, it is clear that uranium(VI) can be selectively removed from the aqueous solutions containing Li^+, Na^+, K^+ and Rb^+ ions. Other inorganic ions such as Th^{4+}, Fe^{3+}, Cu^{2+}, Mg^{2+}, Ca^{2+}, Sr^{2+} and Ba^{2+} could produce hydroxide or carbonate precipitates with OH^- or CO_3^{2-} in the prepared $(NH_4)_4[UO_2(CO_3)_3]$ solution. Thus, the competition adsorption of these ions with UO_2^{2+} on the IIP under this condition were not studied.

Recovery of uranium from seawater

To demonstrate the potential application of the synthesized UO_2^{2+}-IIP, the recovery of UO_2^{2+} from seawater was performed. In the preconcentration experiment, 10 mg IIP was mixed with 10 mL seawater spiked with 30 μg uranium, then was collected and eluted by 10 mL and 50 mmol L^{-1} HCl solution. The concentration of the uranium in the eluent was determined by ICP-AES. As a result, the recovery of uranium was 93.8 ± 5.4 %. It can be seen that the prepared UO_2^{2+}-IIP is able to extract uranium from seawater.

Reusability of the IIP

In order to obtain the reusability of the UO_2^{2+}-IIP, adsorption–desorption cycles were repeated five times by using the same sample. At the 5th cycle, the retention capacity can still maintain 80 % (Fig. 7). It can be concluded that the UO_2^{2+}-IIP is able to be used many times without decreasing their retention capacities significantly.
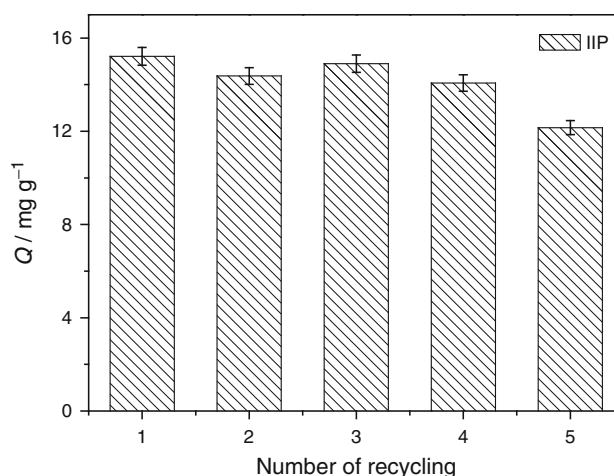

Fig. 7 The retention capacities of the recycled UO_2^{2+}-IIP particles in five times. (Adsorbent: 10 mg, adsorption time: 9 h, uranium concentration: 20 mg L^{-1}, uranium solution: 10 mL, temperature: 25 °C)

Conclusions

A new UO_2^{2+}-IIP was successfully synthesized by using 2,4-dioxopentan-3-yl methacrylate as functional monomer. The IIP exhibited higher adsorption capacity for UO_2^{2+} than CP, and the adsorption kinetics followed the pseudo-second-order kinetic model. Moreover, the IIP could quantitatively separate UO_2^{2+} from other metal ions such as Li^+, Na^+, K^+ and Rb^+. These results indicated that the IIP is able to recognize UO_2^{2+}, i.e., significant imprinting effect. In the sorption process, the polymer particles can compete UO_2^{2+} with CO_3^{2-} in $(NH_4)_4[UO_2(CO_3)_3]$ solution. Furthermore, the IIP can recover uranium from real seawater with an efficiency of * 93 %. Hence, the synthesized UO_2^{2+}-IIP can be used in the extraction of uranium from seawater.

References

1. Annual Report 2011 (2012). International Atomic Energy Agency, Vienna
2. Rao L (2011) Recent international R&D activities in the extraction of uranium from seawater. Lawrence Berkeley National Laboratory
3. Kabay N, Egawa H (1994) Chelating polymers for recovery of uranium from seawater. Sep Sci Technol 29:135–150
4. Duan GJ, Liu TH, Wu WS, Yang Y (2013) Adsorption of UO_2^{2+} from aqueous solution onto copolymers of styrene and maleic anhydride. J Radioanal Nucl Chem 295:2193–2201
5. Tabushi I, Kobuke Y, Nishiya T (1979) Extraction of uranium from seawater by polymer-bound macrocyclic hexaketone. Nature 280:665–666

6. Davies RV, Kennedy J, Hill KM, McIlroy RW, Spence R (1964) Extraction of uranium from sea water. Nature 203:1110–1115

7. Koyanaka Y (1970) Collection of uranium from sea water by galena. J Nucl Sci Technol 7:426–427

8. Krishna PG, Gladis JM, Rao KS, Rao TP, Naidu GRK (2005) Synthesis of xanthate functionalized silica gel and its application for the preconcentration and separation of uranium(VI) from inorganic components. J Radioanal Nucl Chem 266:251–257

9. Ayata S, Merdivan M (2010) *p-tert*-Butylcalix[8]arene loaded silica gel for preconcentration of uranium(VI) via solid phase extraction. J Radioanal Nucl Chem 283:603–607

10. Madrakian T, Afkhami A, Rahimi M (2012) Removal, preconcentration and spectrophotometric determination of U(VI) from water samples using modified maghemite nanoparticles. J Radioanal Nucl Chem 292:597–602

11. Liu YL, Yuan LY, Yuan YL, Lan JH, Li ZJ, Feng YX, Zhao YL, Chai ZF, Shi WQ (2012) A high efficient sorption of U(VI) from aqueous solution using amino-functionalized SBA-15. J Radioanal Nucl Chem 292:803–810

12. Rao TP, Kala R, Daniel S (2006) Metal ion-imprinted polymers—novel materials for selective recognition of inorganics. Anal Chim Acta 578:105–116

13. He FF, Wang HQ, Wang YY, Wang XF, Zhang HS, Li HL, Tang JH (2013) Magnetic Th(IV)-ion imprinted polymers with salophen schiff base for separation and recognition of Th(IV). J Radioanal Nucl Chem 295:167–177

14. Praveen RS, Metilda P, Daniel S, Rao TP (2005) Solid phase extractive preconcentration of uranium(VI) using quinoline-8-ol anchored chloromethylated polymeric resin beads. Talanta 67:960–967

15. Say R, Erosz A, Denizli A (2003) Selective separation of uranium containing glutamic acid molecular-imprinted polymeric microbeads. Sep Sci Technol 38:3431–3447

16. Dai S, Shin YS, Barnes CE, Toth LM (1997) Enhancement of uranyl adsorption capacity and selectivity on silica sol–gel glasses via molecular imprinting. Chem Mater 9:2521–2525

17. James D, Venkateswaran G, Rao TP (2009) Removal of uranium from mining industry feed simulant solutions using trapped amidoxime functionality within a mesoporous imprinted polymer material. Micropor Mesopor Mat 119:165–170

18. Milja TE, Prathish KP, Rao TP (2011) Synthesis of surface imprinted nanospheres for selective removal of uranium from simulants of Sambhar Salt Lake and ground water. J Hazard Mater 188:384–390

19. Sadeghi S, Aboobakri E (2012) Magnetic nanoparticles with an imprinted polymer coating for the selective extraction of uranyl ions. Microchim Acta 178:89–97

20. Singh DK, Mishra S (2009) Synthesis and characterization of UO_2^{2+}-ion imprinted polymer for selective extraction of UO_2^{2+}. Anal Chim Acta 644:42–47

21. Shamsipur M, Fasihi J, Ashtari K (2007) Grafting of ion-imprinted polymers on the surface of silica gel particles through covalently surface-bound initiators: a selective sorbent for uranyl ion. Anal Chem 79:7116–7123

22. Metilda P, Gladis JM, Venkateswaran G, Rao TP (2007) Investigation of the role of chelating ligand in the synthesis of ion-imprinted polymeric resins on the selective enrichment of uranium(VI). Anal Chim Acta 587:263–271

23. Sadeghi S, Mofrad AA (2007) Synthesis of a new ion imprinted polymer material for separation and preconcentration of traces of uranyl ions. React Funct Polym 67:966–976

24. Bae SY, Southard GL, Murray GM (1999) Molecularly imprinted ion exchange resin for purification, preconcentration and determination of UO_2^{2+} by spectrophotometry and plasma spectrometry. Anal Chim Acta 397:173–181

25. Anirudhan TS, Radhakrishnan PG (2009) Improved performance of a biomaterial-based cation exchanger for the adsorption of uranium(VI) from water and nuclear industry wastewater. J Environ Radioactiv 100:250–257

26. Ji XZ, Liu HJ, Wang LL, Sun YK, Wu YW (2013) Study on adsorption of Th(IV) using surface modified dibenzoylmethane molecular imprinted polymer. J Radioanal Nucl Chem 295:265–270

27. Kim H, Kim Y, Chang JY (2012) Preparation of a molecularly imprinted polymer containing europium(III) ions for luminescent sensing. J Polym Sci Polym Chem 50:4990–4994

28. Cejka J, Sejkora J, Plasil J, Bahfenne S, Palmer SJ, Frost RL (2010) Raman spectroscopic study of the uranyl carbonate mineral cejkaite and its comparison with synthetic trigonal $Na_4[UO_2(CO_3)_3]$. J Raman Spectrosc 41:459–464

29. Pakade VE, Cukrowska EM, Darkwa J, Darko G, Torto N, Chimuka L (2012) Simple and efficient ion imprinted polymer for recovery of uranium from environmental samples. Water Sci Technol 65:728–736

30. Khajeh M, Sanchooli E (2010) Development of a selective molecularly imprinted polymer-based solid-phase extraction for copper from food samples. Biol Trace Elem Res 135:325–333

31. Kala R, Gladis JM, Rao TP (2004) Preconcentrative separation of erbium from Y, Dy, Ho, Tb and Tm by using ion imprinted polymer particles via solid phase extraction. Anal Chim Acta 518:143–150

32. Metilda P, Gladis JM, Rao TP (2004) Influence of binary/ternary complex of imprint ion on the preconcentration of uranium(VI) using ion imprinted polymer materials. Anal Chim Acta 512:63–73

33. Biju VM, Gladis JM, Rao TP (2003) Effect of gamma-irradiation of ion imprinted polymer (IIP) particles for the preconcentrative separation of dysprosium from other selected lanthanides. Talanta 60:747–754

34. Ho YS, McKay G (1999) Pseudo-second order model for sorption processes. Process Biochem 34:451–465

35. Liu Y, Liu ZC, Dai JD, Gao J, Xie JM, Yan YS (2011) Selective adsorption of Co(II) by mesoporous silica SBA-15-supported surface ion imprinted polymer: kinetics, isotherms, and thermodynamics studies. Chin J Chem 29:387–398

36. Boonpangrak S, Whitcombe MJ, Prachayasittikul V, Mosbach K, Ye L (2006) Preparation of molecularly imprinted polymers using nitroxide-mediated living radical polymerization. Biosens Bioelectron 22:349–354

37. Favre-Reguillon A, Lebuzit G, Foos J, Guy A, Draye M, Lemaire M (2003) Selective concentration of uranium from seawater by nanofiltration. Ind Eng Chem Res 42:5900–5904

38. Pan JM, Yao H, Guan W, Ou HX, Huo PW, Wang X, Zou XH, Li CX (2011) Selective adsorption of 2,6-dichlorophenol by surface imprinted polymers using polyaniline/silica gel composites as functional support: equilibrium, kinetics, thermodynamics modeling. Chem Eng J 172:847–855